Journal of King Saud University – Science 34 (2022) 101749

Contents lists available at ScienceDirect

Journal of King Saud University – Science

journal homepage: www.sciencedirect.com

Original article

Preparation and antibacterial application of hydroxyapatite doped Silver nanoparticles derived from chicken bone

P. Vijayaraghavan [a,*], M.A. Rathi [b], Khalid S. Almaary [c], Fatima S. Alkhattaf [c], Yahya B. Elbadawi [c], Soon Woong Chang [d], Balasubramani Ravindran [d,*]

[a] Bioprocess Engineering Division, Smykon Biotech, Nagercoil, Kanyakumari, Tamilnadu, 629201, India
[b] Department of Biochemistry, Sree Narayana Guru College, Coimbatore 641 105, Tamil Nadu, India
[c] Department of Botany and Microbiology, College of Science, King Saud University, P.O. 2455, Riyadh 11451, Saudi Arabia
[d] Department of Environmental Energy and Engineering, Kyonggi University Youngtong-Gu, Suwon, Gyeonggi-Do 16227, South Korea

ARTICLE INFO

Article history:
Received 26 October 2021
Revised 20 November 2021
Accepted 29 November 2021
Available online 6 December 2021

Keywords:
Nanoparticles
Green synthesis
Co-precipitation
Hydroxyapatite
Antibacterial

ABSTRACT

Hydroxyapatite was isolated from the chicken bones of Black Sumatra and Fighter cock by thermal calcinations at 700 °C. The reducing power of *Plumbago indica* was responsible for the green synthesis of silver NPs. The isolated hydroxyapatite was used for the preparation of hydroxyapatite doped silver nanoparticles (HAp/AgNPs) against both Gram-positive and Gram-negative bacteria. The Black Sumatra bone derived HAp/AgNPs were excellent activity against *Klebsiella pneumoniae* (28 mm), *Staphylococcus aureus* (26 mm), *Bacillus cereus* (24 mm), respectively. Fighting cock bones derived HAp/AgNPs demonstrated activity against *Staphylococcus aureus* (22 mm), *Klebsiella pneumoniae* (25 mm) and *Bacillus cereus* (23 mm), respectively. The MIC value ranged between 45 ± 1.2 μg/mL and 104 ± 0.25 μg/mL. The HAp/AgNPs were characterized by X-ray diffraction (XRD), Fourier Transformed Infrared spectroscopy (FTIR), and Scanning Electron Microscopy (SEM). The XRD patterns of the Hap/Ag revealed functional peaks representing the reflection planes. The HAp/AgNPs showed an ellipsoidal morphology in SEM analysis. The morphological studies at various magnifications indicated that HAp/AgNPs with good crystal structure could prepared by using co-precipitation method.

1. Introduction

The rapid pace of urbanization and accelerated industrialization is a great challenge for waste management and environmental sustainability (Koop and van Leeuwen, 2016). Elimination of biological wastes requires specific techniques owing to the pathogenic traits, fluid content and their high oxidation rates. Appropriate waste transformation can augment the profit from the by-products and also ensure a sustainable environment. The major contributors of animal wastes are the slaughterhouses; a high percentage of these wastes cannot be converted into value-added by products. The wastes from a slaughter house include bones, skins, feathers, tendons, internal organs and blood depending on the food culture of each region (Adhikari et al., 2018). The fighting cock is a Southeast Asian species that was formerly raised for cockfighting and now one of the most common sources of poultry food. More likely the chickens are reared for their meat and wild chickens that have a life span of 4–6 years have a special price hike in the chicken markets when compared to the broiler chickens that reach a slaughter size within 14 weeks of age (Eda, 2021). The Black Sumatra has lustrous black plumages and the males often engage in fights to mark their dominance. Although the poultry slaughterhouse wastes possess a hazard aspect, handling and processing the wastes can be done efficiently and narrowed down to many applications such as animal feed, chitosan that can be used in dielectric products, gelatine and collagen that are extensively used in cosmetics, medical and pharmaceutical industries (Adhikari et al., 2018). The contemporary methods employ significant approaches to extract compounds from chicken bones that have replaced the traditional methods in dentistry and orthopaedics (Vinoth Kumar et al., 2021).

* Corresponding authors.
E-mail addresses: venzymes@gmail.com (P. Vijayaraghavan), kalamravi@gmail.com (B. Ravindran).
Peer review under responsibility of King Saud University.

Production and hosting by Elsevier

https://doi.org/10.1016/j.jksus.2021.101749
1018-3647/

Hydroxyapatite (HAP) can be extracted from biological sources including mammalian, bovine, fish, cattle and poultry bones. HAP has a key role in stimulating bone regeneration but they can either be deficient in calcium or phosphorous in their non-stoichiometric forms (Shi et al., 2021). HAP synthesized from animal bones can mimic the natural apatite present in human bones and are required to enhance bone formation (Malla et al., 2020). Arrays of techniques are employed for the synthesis of HAP such as thermal treatment, sol–gel method, micro-emulsion technique, chemical-precipitation and hydrothermal approach. HAP prepared using chemical synthesis method does not possess significant biological properties whereas, HAP with desirable biological characteristics synthesized from natural sources in an eco-friendly manner using egg shells and animal bones were biocompatible and exhibited interesting biological activities (Ojo et al., 2021; Yelten-Yilmaz and Yilmaz, 2018). HAP has several applications in the medical and pharmaceutical field including scaffold production in tissue engineering (Shi et al., 2021), yet the amalgamation of HAP with novel materials with multifaceted applications is limited.

Nanotechnology is an emerging field that has grabbed the attention of researchers around the globe and nanomaterials are widely employed in scientific approaches due to their unique properties such as small size, large surface area and target-specific mechanism of action (Kaviyarasu et al, 2020). Metallic-nanoparticles are efficiently synthesized using eco-friendly materials and are comparatively less toxic than nanoparticles synthesized using physical and chemical methods. Plants, microbes and other natural sources are constantly being exploited for the synthesis of nanoparticles that can potentially overcome the threats of toxicity and environmental hazards (Panimalar et al., 2020). However, using wastes to augment the production of nanoparticles can revolutionize the field of nanotechnology by reducing the cost of investment in raw-materials and alternatively reduce environmental pollution and promote sustainability. Amidst other metallic nanoparticles, Silver nanoparticles (AgNPs) have gained the spotlight owing to their exclusive biological properties (Rathnakumar et al., 2019; Amanulla et al., 2018). The antibacterial properties of AgNPs against multidrug resistant strains are interesting and appreciable. Since the search for new antibacterial agents continues due to the upsurge and outbreak of contagious diseases caused by microorganisms and lack of effective antimicrobial agents/antibiotics, pharmaceutical industries and research arenas indulge in developing novel drugs that can effectively tackle antimicrobial resistance (Ciobanu et al., 2012). Silver and gold nanoparticles have antibacterial activities against multi drug resistant bacterial strains detected from various environments (Bindhu et al., 2020; Bindhu and Umadevi, 2014a; Bindhu and Umadevi, 2014b). The emerging problem of multi-drug resistance and the consequences that the food, health and various other sectors stimulate researchers to search effective alternative and safe approaches to fight biofilm formation and antimicrobial resistance. Silver nanoparticles have been widely investigated because of antimicrobial properties. However, recently, it has been recommended to create synergistic composite materials, because bacterial pathogens can effectively develop resistance against metal nanophases; hence, it could be very important to improve and maintain their antibacterial potential. The complex synergistic composite materials comprised AgNPs and one of the active organic molecules (Kukushkina et al., 2021; Uma Maheshwari Nallal et al., 2021). However the use of HAP extracted from chicken bones to prepare HAp/AgNPs has been rarely investigated and its biological properties are uncharted. The emerging trend of the drug resistance development and the consequences that the food, health and other sectors face stimulate biologists to search effective alternative methods to combat drug resistance and biofilm formation. In this study an attempt was made to use *Plumbago indica* for the green synthesis of AgNPs and chicken bone for hydroxyapatite preparation. The main aim of this study is to develop HAp/AgNPs and to investigate synergistic antibacterial properties.

2. Materials and methods

2.1. Preparation of hydroxyapatite from the natural sources

The chicken bones of Black Sumatra and Fighter cock were purchased from a slaughterhouse and washed with tap water several times, followed by distilled water to remove meat and adhered skin and hair on the surface of the bones. Chicken bone was boiled with double distilled water for 1 h and the adhered meat was removed. The bones were broken mechanically and removed bone marrow. It was further treated with acetone for 2 h at 28 ± 1 °C and the bone was washed with double distilled water until the contents on the bones removed. Then it was dried at 80 ± 2 °C for 2 h and the moisture content was removed. The dried chicken bone was ground into small pieces and the bone was placed in silica crucible and calcination process was performed in optimum temperature (700 °C) with adequate holding time as suggested previously (Rajesh et al., 2012; Vinoth Kumar et al., 2021). The schematic presentation of hydroxyapatite preparation was described in Fig. 1.

2.2. Preparation of hydroxyapatite doped silver nanoparticles

2.2.1. Synthesis of AgNPs

P. indica was collected at Kanyakumari, India between January 2021 and February 2021. The aerial part of the plant was removed (100 gm), dried (sun drying) and powdered by mechanical grinding. The powdered material was used for the preparation of nanoparticles. About 1.0 g powder was suspended in 99 mL double distilled water and stirred for 2 h. It was filtered using a Whatman No 1 filter paper and used as the natural bioreductor for the preparation of silver nanoparticles. *Plumbago* extract has been widely used for the green synthesis of nanoparticles due to high phenolic content (Singh et al., 2018). The plant extract (2 mL, 1%) was mixed with aqueous silver nitrate solution (100 mL, 1 mM), followed by microwave assisted green NPs synthesis (Fatimah et al., 2018; Garibo et al., 2020). The development of NPs was monitored using UV–Visible spectra.

2.2.2. Hydroxyapatite doped – silver nanoparticles

The hydroxyapatite doped silver nanoparticles (HAp – AgNPs) was prepared by co-precipitation method. The HAp doped – AgNPs were synthesized from CaO as suggested previously with little modifications from Black Sumatra and Fighting cock with the atomic ratio of Ag/[Ag + Ca] was 0.2. Then it was dissolved in double distilled water (200 mL) and was continuously stirred at room temperature. To the solution, $(NH_4)_2HPO_4$ was continuously added until the atomic ratio of [Ca + Ag]/P was 1.67. It was maintained at 150 °C for overnight in an oven and the final slurry was dried at 80 °C and finally HAp – AgNPs were obtained (Zhou et al., 2020; Ciobanu et al., 2013).

2.3. Antibacterial activity of HAp doped – AgNPs

2.3.1. Bacterial strains

Three Gram-positive bacteria (*Staphylococcus aureus*, *Streptococcus pyogenes* and *Bacillus cereus*) and three Gram-negative bacteria (*Klebsiella pneumoniae*, *Escherichia coli*, and *Enterobacter aerogenes*) were used for the determination of antibacterial activity. The bacteria were sub cultured and transferred to 50 mL Mueller-Hinton broth (MHB) and the culture was incubated for 18 h at 37 ± 1 °C.

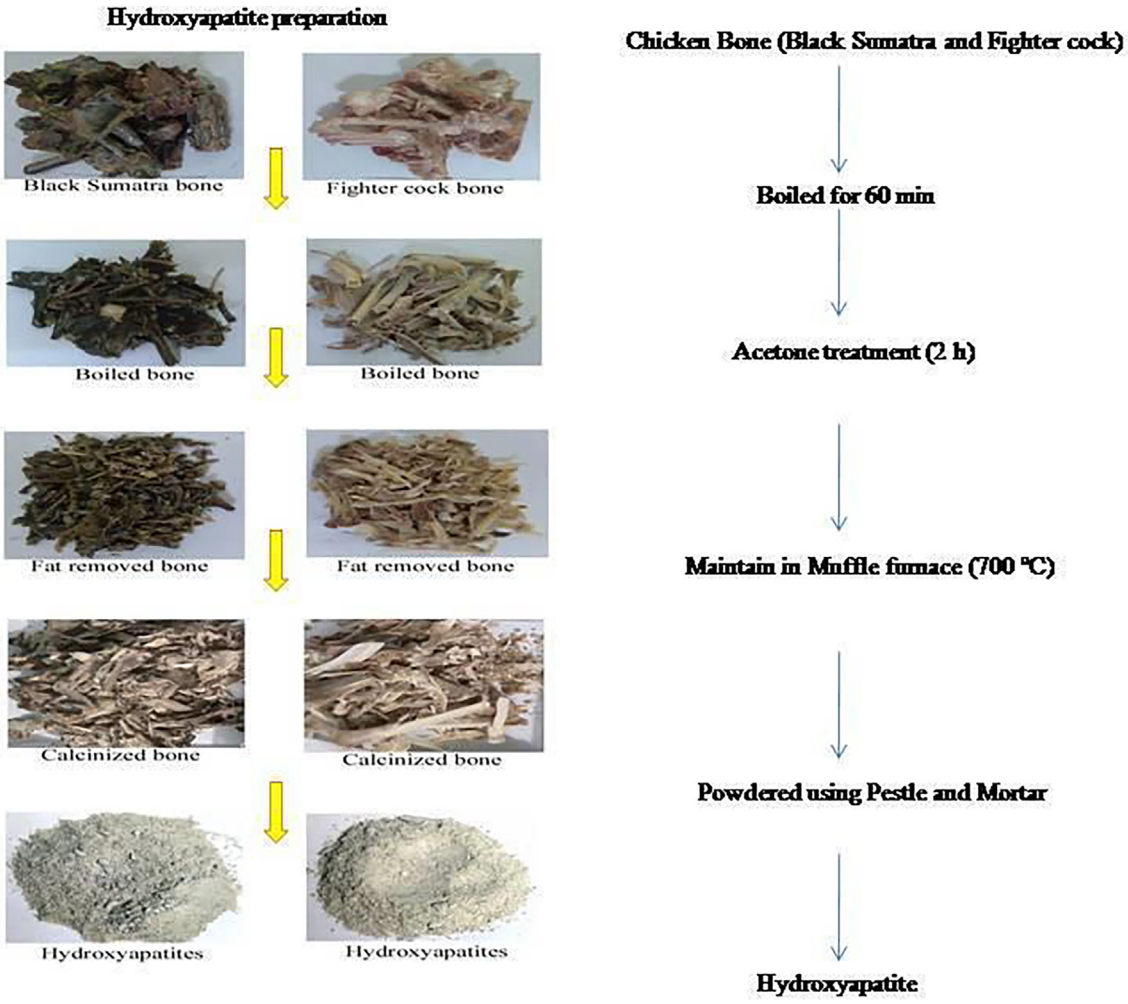

Fig. 1. The schematic presentation of hydroxyapatite preparation.

2.3.2. Disc diffusion method

Gram-positive and Gram-negative bacterial strains were tested for susceptibility to determine antibacterial activity of HAp – AgNPs. Disc diffusion method was used for the determination of antibacterial activity as described previously. The MIC value was determined by analyzing the number of culturable bacterial cells which developed as single colony after in the presence of HAp – AgNPs. Overnight culture of Gram-positive and Gram-negative bacterial strains were cultured in 100 mL Erlenmeyer flask containing 50 mL LB broth medium and incubated at 37 ± 1 °C at 150-rpm for 24 h at various concentrations of HAp – AgNPs. The growth of bacteria was visually analyzed after 24 h and the minimum inhibitory concentration (MIC) was determined as described earlier.

2.3.3. Characterization of HAp – AgNPs

CaO prepared from Black Sumatra mediated particles (HAp – AgNPs) were used for structural characterization. The morphology of HAp – AgNPs microparticles was analyzed using a Scanning Electron Microscopy (SEM, S 4800) operated at 5 kV with 2.4Kx, 5Kx, 12Kx and 25 Kx magnification. The FT-IR spectrum of the sample was registered from 500 to 4500 cm^{-1} on dried KBr pellets using Fourier Transform Infrared analysis. The crystalline nature and lattice factors of HAp – AgNPs were analyzed using XRD analysis.

3. Results

3.1. Extraction of natural hydroxyapatite

Black Sumatra and Fighter cock bones were suitable source of hydroxyapatite. The colour of the Black Sumatra cock bone was black after deproteination, whereas the fighting cock bone was thin pale yellow in colour. The yield of the deproteinized bone of Black Sumatra and Fighting cock was 25 g, 19 g, respectively. The deproteinized bone was subjected to thermal treatment at 700 ○C and a colourless (white) crystalline powder was obtained.

3.2. Antimicrobial activity of HAp – AgNPs against Gram-positive and Gram-negative bacteria

The bacteria such as, *S. aureus*, *S. pyogenes*, *B. cereus*, *K. pneumoniae*, *E. coli*, and *E. aerogenes* were selected to investigate the mechanism of action because of different cell structures. From the inhibitory zone on MHA plates, it can be evidenced that the analyzed HAp – AgNPs showed potent bactericidal activity on both Gram-negative and Gram-positive strains. From the results, it can be seen that the Black Sumatra bone derived HAp – AgNPs were excellent activity against *K. pneumoniae* (28 mm), *S. aureus* (26 mm), *B. cereus* (24 mm), respectively. Fighting cock bones

derived silver HAp – AgNPs demonstrated activity against *S. aureus* (22 mm), *K. pneumoniae* (25 mm) and *B. cereus* (23 mm), respectively (Fig. 2). The MIC value ranged between 45 ± 1.2 μg/mL and 104 ± 0.25 μg/mL (Table 1). It is also to be explained that Black Sumatra bone derived HAp – AgNPs showed excellent antibacterial activity than Fighter cock, hence further characterization experiments were performed only with Black Sumatra bone derived HAp – AgNPs. Hydroxyapatite-Ag composite materials have the ability to affect biofilm formation and antimicrobial resistance. These synergistic composite materials have activity against both Gram-positive and Gram-negative bacterial pathogens and the result was compared with other fabricated materials (Table 2).

Table 1
Minimum inhibitory concentration of chicken bone derived HAp/AgNPs against Gram-positive and Gram-negative bacteria.

Bacteria	Minimum Inhibitory Concentration (μg/mL)	
	Black Sumatra-HAP-AgNPs	Fighter Cock-HAP-AgNPs
S. aureus	45 ± 1.2	49 ± 2.5
K. pneumoniae	49.5 ± 3.1	53 ± 1.8
S. pyogenes	63 ± 2.5	68 ± 0.35
E. coli	72 ± 0.5	79 ± 2.5
B. cereus	46 ± 1.25	68 ± 1.25
E. aerogenes	89 ± 5	104 ± 0.128

3.3. Doping and characterization of HAp – AgNPs

The colour of the green synthesized AgNPs was changed from a pale yellow to a deep brown colour after 10 min microwave assisted bioreduction indicating the development of AgNPs. The reducing power of *P. indica* extract is mainly due to the presence of phenolic compound in the extract. The XRD patterns of HAp – AgNPs described in Fig. 2 revealed functional peaks characteristics of HA at 2θ values of 18.2°, 23°, 26.8°, 32.4°, 39.1°, 42.8°, 47.6°, 49.2°, 57.2°, 62.3° and 79.2°, representing the reflection planes (001), (002), (111), (211), (110), (301), (200), (222), (004), (322) and (313), respectively (Fig. 3). From the above results, the reflection (211) was for HAp – AgNPs and (200) for Ag crystal lattice, respectively. The present finding demonstrated suitability of Black Sumatra bone to produce HA with appreciated level of crystallinity. The characteristic reflections were noticed for HAp – AgNPs. The HAp – AgNPs samples showed open-porous structure which indicated higher porosity and this porosity was developed because of sintering process. FT-IR spectrum of HAp – AgNPs revealed intense band and symmetric stretching. The sharp and intense band at 554 cm^{-1} and 1074 cm^{-1} revealed symmetric stretching of –P-O. The broad band at 3405 cm^{-1} revealed the presence of –OH group. The bands occurred in the spectra of 1415, 1634 and 2354 cm^{-1} (Fig. 4). As described in Fig. 5, the doped HAp-Ag nanoparticles showed an ellipsoidal morphology in SEM analysis. The morphological studies at various magnifications indicated good crystal structure of HAp – AgNPs and co-precipitation is one of the suitable methods for the preparation of HAp – AgNPs.

4. Discussion

Natural HAp was isolated from chicken bone of Black Sumatra and Fighting cock at optimized temperature (700 °C) and yielded white crystalline powder from both bones. The colour and the yield of HAp were comparable with previous studies on waste chicken bone of other breeds (Rajesh et al., 2012). The colour of the HAp was related to sintering temperature and time of bone. In the case of HAp preparation from bones, sintering time was mainly related to the availability of ash content as a consequence of incomplete organic combustion in the bone sample of chicken. Appearance of white colour at 700 °C indicated complete calcinations. The present finding and previous results reported by Rajesh et al. (2012) revealed prolonged and low temperature for better calcinations (Ramirez-Gutierrez et al., 2017). XRD analysis revealed diffractogram of calcined bone sample heated at 700 °C.

In this study, the chicken bone treated at 700 °C of thermal treatment sharply increased the diffraction peaks and this is attributed to the strong elimination of various amorphous organic substances from the sample. It has been previously reported a narrower and sharper diffractogram peak in various calcinated samples at high thermal treatment deduces the maximum crystallinity in the treated human and animal bone (Figueiredo et al., 2010). At lower thermal treatment, the presence of inorganic ions

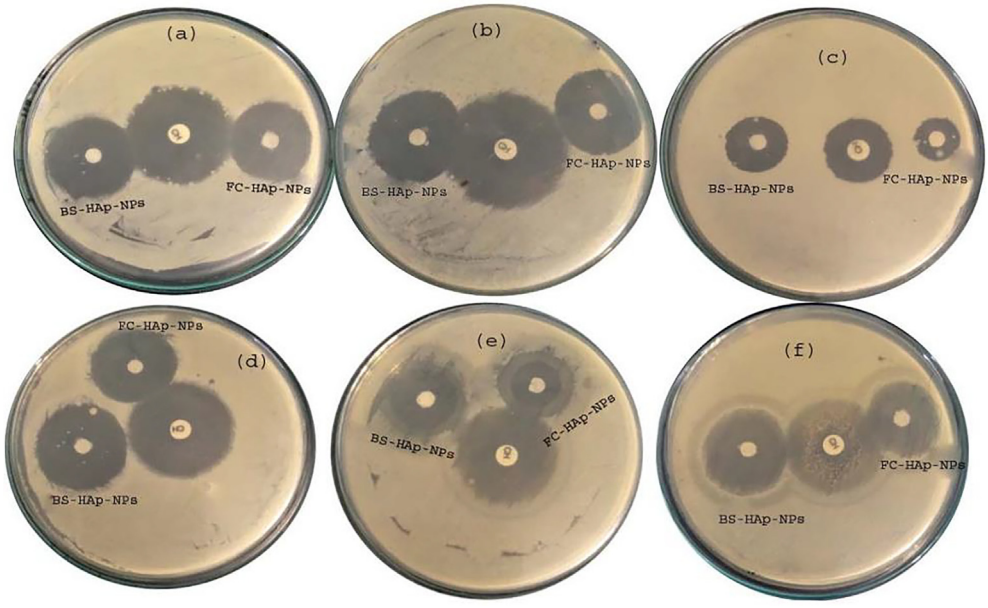

Fig. 2. Antibacterial activity of HAp/AgNPs against Gram-positive and Gram-negative bacteria (a: *K. pneumoniae*; b: *E. coli*; c: *E. aerogenes*; d: *S. aureus*; e: *S. pyogenes* and g: *B. cereus*).

Table 2
Biological activity of AgNPs-composite materials prepared by various methods.

Nature of the composite material	Method	Size (nm)	Susceptible bacteria	Reference
Silver-doped hydroxyapatite	Coprecipitation	5 –15	*K. pneumoniae, C. krusei* 963	Costescu et al., 2013
Silver doped hydroxyapatite	Sol-gel method	25	*E. coli, S. aureus*	Jadalannagari et al., 2014
Silver-doped hydroxyapatite	Sol-gel dip coating	100	*S. aureus* 0364, *E. coli* ATCC 25,922	Predoi et al., 2016
Silver-hydroxyapatite	Co-precipitation	100	*S. aureus, Pneumococcus*	Díaz et al., 2009
Hydroxyapatite-Ag composite	Adsorption	22.03	*P. aeruginosa, E. coli*	Silva-Holguín and Reyes-López, 2020
Silver nanoparticle-doped hydroxyapatite	Co-precipitation	550	*E. coli, S. aureus.*	Zhou et al., 2020
Silver-doped hydroxyapatite	sol-Gel Spin Coating	21 ± 1.7	*Candida albicans*	Prodan et al., 2020
Silver nanoparticle-doped hydroxyapatite	Coprecipitation	4–12	*E. coli, K. pneumoniae*	Citradewi et al., 2021
Silver-hydroxyapatite	One-pot method	20–40	*S. mutans*	Hou et al., 2021
Hydroxyapatite-Ag composite	Coprecipitation	20–30	*K. pneumoniae, S. aureus*	Present study

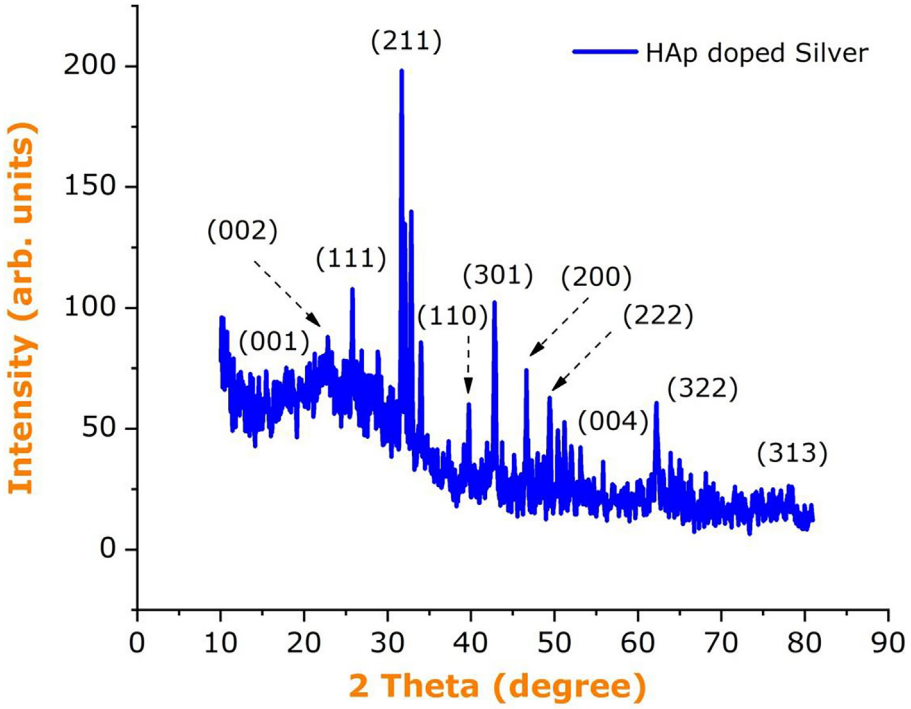

Fig. 3. XRD pattern for Black Sumatra chicken bone derived plant mediated HAp/AgNPs.

such as, CO_3^{2+} and Mg^{2+} were determined in the bone samples, and these minerals leads to the destabilization and distortion of HA structure, hence optimum thermal dissociation at higher calcinations temperature and is preferred for better stable HAp lattice (Tõnsuaadu et al., 2012). The XRD patterns of doped NPs revealed the presence of characteristics peak at better reflection plates and these are similar with previous reports (Reddy et al., 2007; Türk et al., 2017). The reflection (111) and (200) revealed the presence of Ag crystal lattice in the XRD analysis and this has been previous reported (Hassan et al., 2021; Silva-Holguín and Reyes-López, 2020). The antibacterial activity of HAp – AgNPs was analyzed using various human pathogenic bacteria. Nanoparticles have large surface area with bacterial cells and, hence a good interaction with the bacterial target will occur. The inhibitory effect of NPs varied based on the size of the NPs (Raimondi et al., 2005). Plant extracts have been previously used for the green synthesis of silver and gold nanoparticles and the complex synergistic composite materials showed antimicrobial properties (Bindhu and Umadevi, 2015; Bindhu et al., 2014; Bindhu and Umadevi, 2013). Hydroxyapatite doped silver nanoparticles were excellent activity against *Klebsiella pneumoniae* (28 mm), *Staphylococcus aureus* (26 mm), *Bacillus cereus* (24 mm), respectively. The antimicrobial properties of gold and silver composite materials have been demonstrated previously. The synthesized silver, gold, and palladium composite materials were active against various drug resistant Gram-positive and Gram-negative bacterial strains (Anjana et al., 2019). Green synthesised NPs and preparation of composite materials using organic sources add additional advantages. *Solanum lycopersicums* fruit extract has been used for the green synthesis of silver nanoparticles and capping agent. These green synthesized nanoparticles have various biological activities, including antibacterial and antifungal activities (Umadevi et al., 2013). About 12.5 μg spherical shaped silver NPs is required to kill bacteria, whereas about 50–100 μg of silver ions at increased size (Pal et al., 2007). The activity of HAp – AgNPs varied based on the silver concentration and shape of the composite materials. Ciobanu et al. (2013) reported antimicrobial properties of silver doped hydroxyapatite NPs against Gram-positive, Gram-negative and fungal pathogens. Gram-positive and Gram-negative bacterial strains have been selected to determine the interactive effect based on cell wall. The doped NPs showed antibacterial activity on the Gram-negative and Gram-positive bacterial strains. However, Gram-negative bacteria was highly susceptible than Gram-positive bacteria and the bactericidal activity has been described

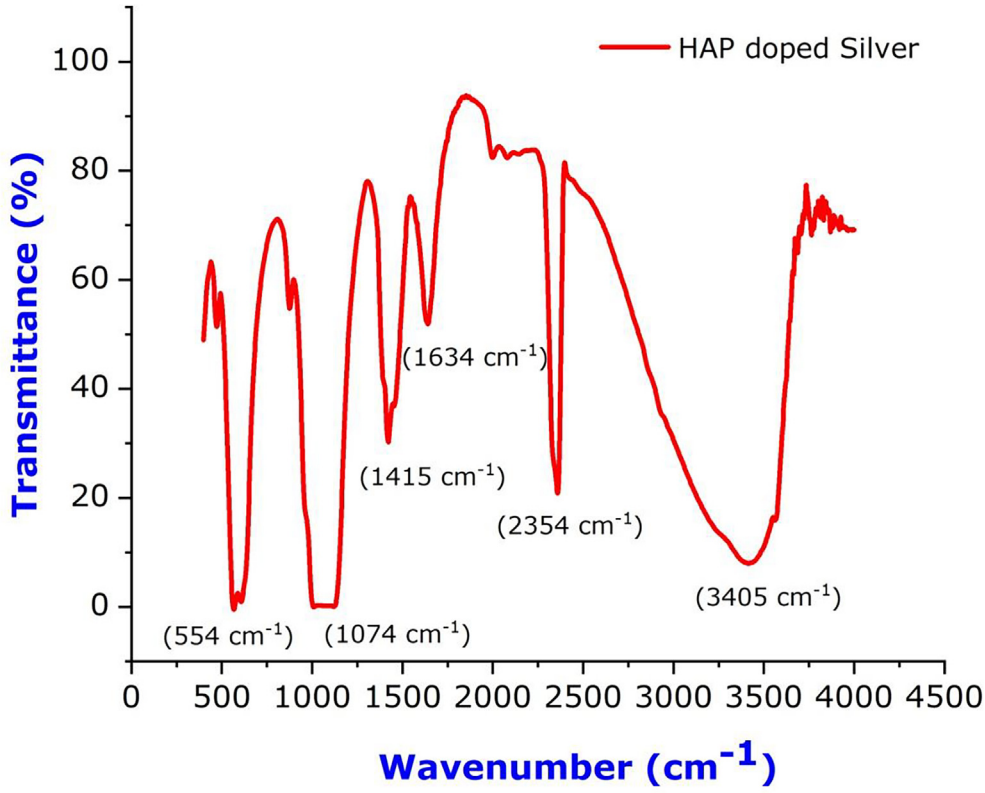

Fig. 4. FTIR spectrum for chicken bone derived plant mediated HAp/AgNPs.

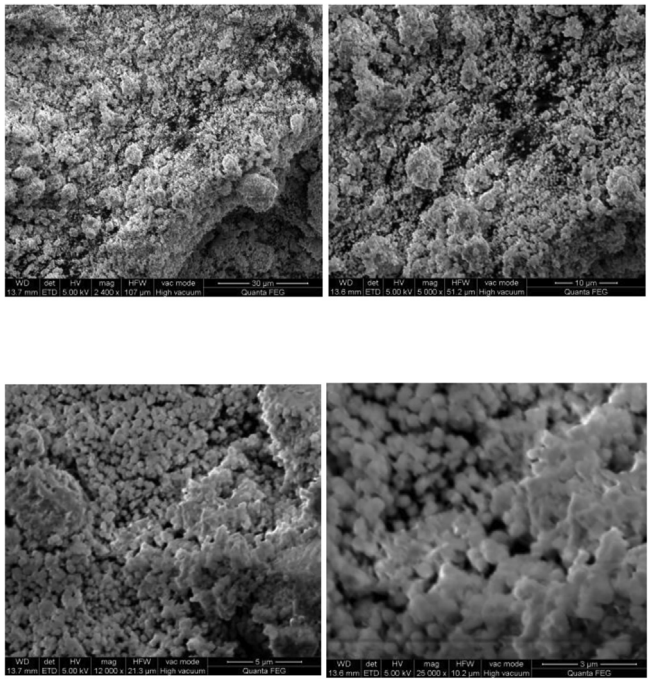

Fig. 5. Scanning Electron Microscopy images of HAp/AgNPs (2400X, 5000X, 12000X and 25,000 X).

previously (Franci et al., 2015). The ionic form of Ag/HAs disrupts the bacteria cell wall and binds to RNA and DNA and inhibits bacterial replication (Kolanthai et al., 2017; Liu et al., 2013).

Morphological studies were performed by SEM imaging at various magnifications. The calcinated chicken bone analyzed in this study revealed spheroidal-like structure with various porosities. At higher temperatures, the inter-granular holes of the bones are more apparent and the grain size increased at higher sintering temperatures. This increased size can be achieved as the result of decarbonation and decomposition process in the HA lattice and increased temperature improved the growth of HA structure (Ramirez-Gutierrez et al., 2017). The SEM analysis revealed the presence of uniform sized HAs from chicken bone and revealed the presence of open porous structure. The increased porosity of the sample derived from bone showed similarity to the previous findings indicated the influence of sintering process (Ciobanu et al., 2014; Hassan et al., 2021). In this study, the absorbance peak was observed in the region between 1600 and 1700 cm^{-1} revealed to O–H bending which confirmed absorption of water by the synthesized materials (Kreibig and Vollmer, 1995; Predoi et al., 2007). The XRD results of HAp – AgNPs revealed that powders prepared by co-precipitation did not show any impurities and this result was in accordance the observations made previously (Ciobanu et al., 2012). In the XRD patterns, absence of various other phases of HAp – AgNPs in bones sample revealed that the silver ions have substituted with HAPs without affecting the crystal structure of the HAp. This result was in accordance the observations made previously by Ravindran et al. (2010). The morphological analysis of HAp – AgNPs revealed good crystal structure and are useful for various applications.

5. Conclusions

In this study, chicken bone was used for the extraction of Hydroxyapatite. The bioprocessing of naturally available biowaste is useful to reduce environmental pollution. The thermal calcinations treatment was effective at 700 °C and results revealed the absence of any organic matter at this thermal temperature. The

analyzed HAp – AgNPs showed potent bactericidal activity on both Gram-negative and Gram-positive strains. The doped HAp – AgNPs revealed an ellipsoidal morphology in SEM analysis. The structural analysis of composite materials revealed good crystal structure and are useful for various applications. Further, the material exhibited promising activity towards anti adipogenic activities against the cell lines, therefore, further studies are in progress.

Declaration of Competing Interest

The authors declare that they have no known competing financial interests or personal relationships that could have appeared to influence the work reported in this paper.

Acknowledgement

The authors thank, Bioprocess Engineering Division, Smykon Biotech PvT LtD, Nagercoil, for providing the facility to perform the experiment. The authors extend their appreciation to the Researchers supporting project number (RSP-2021/189), King Saud University, Riyadh, Saudi Arabia. The authors thank, Kyonggi University laboratory for performing the spectral analysis of the samples.

References

Adhikari, B.B., Chae, M., Bressler, D.C., 2018. Utilization of slaughterhouse waste in value-added applications: recent advances in the development of wood adhesives. Polymer 10, 176. https://doi.org/10.3390/POLYM10020176.

Amanulla, A.M., Shahina, S.J., Sundaram, R., Magdalane, C.M., Kaviyarasu, K., Letsholathebe, D., Mohamed, S.B., Kennedy, J., Maaza, M., 2018. Antibacterial, magnetic, optical and humidity sensor studies of β-CoMoO4-Co3O4 nanocomposites and its synthesis and characterization. J. Photochem. Photobiol B. Biol. 183, 233–241. https://doi.org/10.1016/j.jphotobiol.2018.04.034.

Anjana, P.M., Bindhu, M.R., Umadevi, M., Rakhi, R.B., 2019. Antibacterial and electrochemical activities of silver, gold, and palladium nanoparticles dispersed amorphous carbon composites. Appl. Surface Sci. 479, 96–104. https://doi.org/10.1016/j.apsusc.2019.02.057.

Bindhu, M.R., Umadevi, M., Esmail, G.A., Al-Dhabi, N.A., Arasu, M.V., 2020. Green synthesis and characterization of silver nanoparticles from *Moringa oleifera* flower and assessment of antimicrobial and sensing properties. J. Photochem. Photobiol. B: Biol. 205, 111836. https://doi.org/10.1016/j.jphotobiol.2020.111836.

Bindhu, M.R., Umadevi, M., 2014a. Silver and gold nanoparticles for sensor and antibacterial applications. Spectrochim. Acta Part A: Mol. Biomol. Spectroscopy 128, 37–45. https://doi.org/10.1016/j.saa.2014.02.119.

Bindhu, M.R., Umadevi, M., 2014b. Surface plasmon resonance optical sensor and antibacterial activities of biosynthesized silver nanoparticles. Spectrochim. Acta Part A: Mol. Biomol. Spectroscopy 121, 596–604. https://doi.org/10.1016/j.saa.2013.11.019.

Bindhu, M.R., Umadevi, M., 2015. Antibacterial and catalytic activities of green synthesized silver nanoparticles. Spectrochim. Acta Part A: Mol. Biomol. Spectroscopy 135, 373–378. https://doi.org/10.1016/j.saa.2014.07.045.

Bindhu, M.R., Rekha, P.V., Umamaheswari, T., Umadevi, M., 2014. Antibacterial activities of Hibiscus cannabinus stem-assisted silver and gold nanoparticles. Mat. Lett. 131, 194–197. https://doi.org/10.1016/j.matlet.2014.05.172.

Bindhu, M.R., Umadevi, M., 2013. Synthesis of monodispersed silver nanoparticles using Hibiscus cannabinus leaf extract and its antimicrobial activity. Spectrochim. Acta Part A: Mol. Biomol. Spectroscopy 101, 184–190. https://doi.org/10.1016/j.saa.2012.09.031.

Ciobanu, C.S., Iconaru, S.L., Chifiriuc, M.C., Costescu, A., Le Coustumer, P., Predoi, D., 2013. Synthesis and antimicrobial activity of silver-doped hydroxyapatite nanoparticles. Biomed Res. Int. 2013, 1–10. https://doi.org/10.1155/2013/916218.

Ciobanu, C.S., Iconaru, S.L., Le Coustumer, P., Constantin, L.V., Predoi, D., 2012. Antibacterial activity of silver-doped hydroxyapatite nanoparticles against gram-positive and gram-negative bacteria. Nanoscale Res. Lett. 71, 1–9. https://doi.org/10.1186/1556-276X-7-324.

Ciobanu, G., Ilisei, S., Luca, C., 2014. Hydroxyapatite-silver nanoparticles coatings on porous polyurethane scaffold. Mater. Sci. Eng. C 35, 36–42. https://doi.org/10.1016/J.MSEC.2013.10.024.

Citradewi, P.W., Hidayat, H., Purwiandono, G., Fatimah, I.s., Sagadevan, S., 2021. Clitorea ternatea-mediated silver nanoparticle-doped hydroxyapatite derived from cockle shell as antibacterial material. Chem. Phy. Lett. 769, 138412. https://doi.org/10.1016/j.cplett.2021.138412.

Costescu, A., Ciobanu, C.S., Iconaru, S.L., Ghita, R.V., Chifiriuc, C.M., Marutescu, L.G., Predoi, D., 2013. Fabrication, characterization, and antimicrobial activity, evaluation of low silver concentrations in silver-doped hydroxyapatite nanoparticles. J. Nanomat. 2013, 1–9. https://doi.org/10.1155/2013/194854.

Díaz, M., Barba, F., Miranda, M., Guitián, F., Torrecillas, R., Moya, J.S., 2009. Synthesis and antimicrobial activity of a silver-hydroxyapatite nanocomposite. J. Nanomat. 2009, 1–6. https://doi.org/10.1155/2009/498505.

Eda, M., 2021. Origin of the domestic chicken from modern biological and zooarchaeological approaches. Anim. Front. 11, 52–61. https://doi.org/10.1093/AF/VFAB016.

Fatimah, I.s., Aulia, G.R., Puspitasari, W., Nurillahi, R., Sopia, L., Herianto, R., 2018. Microwave-synthesized hydroxyapatite from paddy field snail (*Pila ampullacea*) shell for adsorption of bichromate ion. Sustain. Environ. Res. 28 (6), 462–471.

Figueiredo, M., Fernando, A., Martins, G., Freitas, J., Judas, F., Figueiredo, H., 2010. Effect of the calcination temperature on the composition and microstructure of hydroxyapatite derived from human and animal bone. Ceram. Int. 36 (8), 2383–2393.

Franci, G., Falanga, A., Galdiero, S., Palomba, L., Rai, M., Morelli, G., Galdiero, M., 2015. Silver nanoparticles as potential antibacterial agents. Molecules 20, 8856–8874. https://doi.org/10.3390/MOLECULES20058856.

Garibo, D., Borbón-Nuñez, H.A., de León, J.N.D., García Mendoza, E., Estrada, I., Toledano-Magaña, Y., Tiznado, H., Ovalle-Marroquin, M., Soto-Ramos, A.G., Blanco, A., Rodríguez, J.A., Romo, O.A., Chávez-Almazán, L.A., Susarrey-Arce, A., 2020. Green synthesis of silver nanoparticles using Lysilomaacapulcensis exhibit high-antimicrobial activity. Sci. Rep. 101, 1–11. https://doi.org/10.1038/s41598-020-69606-7.

Hassan, A.A., Radwan, H.A., Abdelaal, S.A., Al-Radadi, N.S., Ahmed, M.K., Shoueir, K. R., Hady, M.A., 2021. Polycaprolactone based electrospun matrices loaded with Ag/hydroxyapatite as wound dressings: morphology, cell adhesion, and antibacterial activity. Int. J. Pharm. 593, 120143. https://doi.org/10.1016/j.ijpharm.2020.120143.

Hou, J., Liu, Y., Han, Z., Song, D., Zhu, B., 2021. Silver-hydroxyapatite nanocomposites prepared by three sequential reaction steps in one pot and their bioactivities *in vitro*. Mat. Sci. Eng. C 120, 111655. https://doi.org/10.1016/j.msec.2020.111655.

Jadalannagari, S., Deshmukh, K., Ramanan, S.R., Kowshik, M., 2014. Antimicrobial activity of hemocompatible silver doped hydroxyapatite nanoparticles synthesized by modified sol–gel technique. Appl. Nanosci. 4 (2), 133–141.

Kaviyarasu, K., Magdalane, C.M., Jayakumar, D., Samson, Y., Bashir, A.K.H., Maaza, M., Letsholathebe, D., Mahmoud, A.H., Kennedy, J., 2020. High performance of pyrochlore like Sm2Ti2O7 heterojunction photocatalyst for efficient degradation of rhodamine-B dye with waste water under visible light irradiation. J. King Saud. Univ-Sci. 32 (2), 1516–1522. https://doi.org/10.1016/j.jksus.2019.12.006.

Kolanthai, E., AbinayaSindu, P., Thanigai Arul, K., Sarath Chandra, V., Manikandan, E., Narayana Kalkura, S., 2017. Agarose encapsulated mesoporous carbonated hydroxyapatite nanocomposites powder for drug delivery. J. Photochem. Photobiol. B Biol. 166, 220–231. https://doi.org/10.1016/J.JPHOTOBIOL.2016.12.005.

Koop, S.H.A., van Leeuwen, C.J., 2016. The challenges of water, waste and climate change in cities. Environ. Dev. Sustain. 19 (2), 385–418.

Kreibig, U., Vollmer, M., 1995. Theoretical considerations. Opt. Prop. Met. Clust. 25, 13–201. https://doi.org/10.1007/978-3-662-09109-8_2.

Kukushkina, E.A., Hossain, S.I., Sportelli, M.C., Ditaranto, N., Picca, R.A., Cioffi, N., 2021. Ag-based synergistic antimicrobial composites. A critical review. Nanomaterials 11 (7), 1687. https://doi.org/10.3390/nano11071687.

Liu, X., Mou, Y., Wu, S., Man, H.C., 2013. Synthesis of silver-incorporated hydroxyapatite nanocomposites for antimicrobial implant coatings. Appl. Surf. Sci. 273, 748–757. https://doi.org/10.1016/J.APSUSC.2013.02.130.

Malla, K.P., Regmi, S., Nepal, A., Bhattarai, S., Yadav, R.J., Sakurai, S., Adhikari, R., 2020. Extraction and characterization of novel natural hydroxyapatite bioceramic by thermal decomposition of waste ostrich bone. Int. J. Biomater. 2020, 1–10. https://doi.org/10.1155/2020/1690178.

Ojo, O.E., Sekunowo, I.O., Ilomuanya, M.O., Gbenebor, P.O., Adeosun, S.O., 2021. Compositions and thermo-chemical analysis of bovine and caprine bones. Kufa J. Eng. 12 (3), 56–68.

Pal, S., Tak, Y.K., Song, J.M., 2007. Does the antibacterial activity of silver nanoparticles depend on the shape of the nanoparticle? a study of the gram-negative bacterium *Escherichia coli*. Appl. Environ. Microbiol. 73 (6), 1712–1720. https://doi.org/10.1128/AEM.02218-06.

Panimalar, S., Uthrakumar, R., Selvi, E.T., Gomathy, P., Inmozhi, C., Kaviyarasu, K., Kennedy, J., 2020. Studies of MnO2/g-C3N4 hetrostructure efficient of visible light photocatalyst for pollutants degradation by sol-gel technique. Surface. Interface. 20, 100512. https://doi.org/10.1016/j.surfin.2020.100512.

Predoi, D., Andronescu, E., Costache, M., Predoi, D., Barsan, M., Andronescu, E., Vatasescu-Balcan, R.A., Costache, M., 2007. Hydroxyapatite-iron oxide bioceramic prepared using nano-size powders Quantum Optical Lithography View project Petabyte Optical Disc View project Hydroxyapatite-iron oxide bioceramic prepared using nano-size powders. Artic. J. Optoelectron. Adv. Mater. 9, 3609–3613.

Predoi, D., Popa, C.L., Chapon, P., Groza, A., Iconaru, S.L., 2016. Evaluation of the antimicrobial activity of different antibiotics enhanced with silver-doped hydroxyapatite thin films. Materials 9 (9), 778. https://doi.org/10.3390/ma9090778.

Prodan, A.M., Iconaru, S.L., Predoi, M.V., Predoi, D., Motelica-Heino, M., Turculet, C.S., Beuran, M., 2020. Silver-doped hydroxyapatite thin layers obtained by sol-gel

spin coating procedure. Coatings 10 (1), 14. https://doi.org/10.3390/coatings10010014.
Raimondi, F., Scherer, G.G., Kötz, R., Wokaun, A., 2005. Nanoparticles in energy technology: examples from electrochemistry and catalysis. Angew. Chemie Int. Ed. 44 (15), 2190–2209.
Rajesh, R., Hariharasubramanian, A., Ravichandran, Y.D., 2012. Chicken Bone as a Bioresource for the Bioceramic (Hydroxyapatite). http://dx.doi.org/10.1080/10426507.2011.650806 187, 914–925.
Ramirez-Gutierrez, C.F., Londoño-Restrepo, S.M., del Real, A., Mondragón, M.A., Rodriguez-García, M.E., 2017. Effect of the temperature and sintering time on the thermal, structural, morphological, and vibrational properties of hydroxyapatite derived from pig bone. Ceram. Int. 43 (10), 7552–7559.
Rathnakumar, S.S., Noluthando, K., Kulandaiswamy, A.J., Rayappan, J.B.B., Kasinathan, K., Kennedy, J., Maaza, M., 2019. Stalling behaviour of chloride ions: a non-enzymatic electrochemical detection of α-Endosulfan using CuO interface. Sensor Actuat. B. Chem. 293, 100–106. https://doi.org/10.1016/j.snb.2019.04.141.
Ravindran, A., Singh, A., Raichur, A.M., Chandrasekaran, N., Mukherjee, A., 2010. Studies on interaction of colloidal Ag nanoparticles with Bovine Serum Albumin (BSA). Colloids Surfaces B Biointerfaces 76 (1), 32–37.
Reddy, M., Venugopal, A., Subrahmanyam, M., 2007. Hydroxyapatite photocatalytic degradation of calmagite (an azo dye) in aqueous suspension. Appl. Catal. B Environ. 69 (3-4), 164–170.
Shi, H., Zhou, Z., Li, W., Fan, Y., Li, Z., Wei, J., 2021. Hydroxyapatite based materials for bone tissue engineering: a brief and comprehensive introduction. Cryst. 11, 149. https://doi.org/10.3390/CRYST11020149.
Silva-Holguín, P.N., Reyes-López, S.Y., 2020. Synthesis of hydroxyapatite-Ag composite as antimicrobial agent: https://doi.org/10.1177/1559325820951342 18. https://doi.org/10.1177/1559325820951342.
Singh, K., Naidoo, Y., Mocktar, C., Baijnath, H., 2018. Biosynthesis of silver nanoparticles using *Plumbago auriculata* leaf and calyx extracts and evaluation of their antimicrobial activities. Adv. Nat. Sci. Nanosci. Nanotechnol. 9 (3), 035004. https://doi.org/10.1088/2043-6254/aad1a3.
Tõnsuaadu, K., Gross, K.A., Plüduma, L., Veiderma, M., 2012. A review on the thermal stability of calcium apatites. J. Therm. Anal. Calorim. 110 (2), 647–659.
Türk, S., Altınsoy, İ., ÇelebiEfe, G., Ipek, M., Özacar, M., Bindal, C., 2017. Microwave–assisted biomimetic synthesis of hydroxyapatite using different sources of calcium. Mater. Sci. Eng. C 76, 528–535.
Umadevi, M., Bindhu, M.R., Sathe, V., 2013. A novel synthesis of malic acid capped silver nanoparticles using Solanum lycopersicums fruit extract. J. Mat. Sci. Technol. 29 (4), 317–322. https://doi.org/10.1016/j.jmst.2013.02.002.
Uma Maheshwari Nallal, V., Prabha, K., VethaPotheher, I., Ravindran, B., Baazeem, A., Chang, S.W., Otunola, G.A., Razia, M., 2021. Sunlight-driven rapid and facile synthesis of Silver nanoparticles using Allium ampeloprasum extract with enhanced antioxidant and antifungal activity. Saudi J. Biol. Sci. 28 (7), 3660–3668.
Vinoth Kumar, K.C., Jani Subha, T., Ahila, K.G., Ravindran, B., Chang, S.W., Mahmoud, A.H., Mohammed, O.B., Rathi, M.A., 2021. Spectral characterization of hydroxyapatite extracted from Black Sumatra and Fighting cock bone samples: A comparative analysis. Saudi J. Biol. Sci. 28 (1), 840–846.
Yelten-Yilmaz, A., Yilmaz, S., 2018. Wet chemical precipitation synthesis of hydroxyapatite (HA) powders. Ceram. Int. 44 (8), 9703–9710.
Zhou, Q., Wang, T., Wang, C., Wang, Z., Yang, Y., Li, P., Cai, R., Sun, M., Yuan, H., Nie, L., 2020. Synthesis and characterization of silver nanoparticles-doped hydroxyapatite/alginate microparticles with promising cytocompatibility and antibacterial properties. Coll. Surface. A: Physicochem. Eng. Aspect. 585, 124081. https://doi.org/10.1016/j.colsurfa.2019.124081.